Journal of Materials Chemistry A

Accepted Manuscript

ROYAL SOCIETY OF CHEMISTRY

www.rsc.org/materialsA

Journal of Materials Chemistry A RSCPublishing

ARTICLE

Improved AlPO-18 membranes for light gas separations

Cite this: DOI: 10.1039/xoxxoooooox

Bin Wang,[a,b] Na Hu,[b] Huamei Wang,[b] Yihong Zheng,[b] Rongfei Zhou *[a,b]

Received ooth February 2015,
Accepted ooth 2015

DOI: 10.1039/xoxxoooooox

www.rsc.org/

High-quality AlPO-18 membranes were synthesized using lost-cost symmetric alumina supports by a single hydrothermal step, and showed to be useful for light gas separations. Single-gas permeances of CO_2, N_2, CH_4 and C_3H_8 decreased with increasing kinetic diameter. Single CO_2 and CH_4 permeances dependence of pressure drop were predicted by Maxwell-Stefan diffusion model and were in agreement with experimental data. The best membranes showed smaller-component permeances of 6.5, 6.3 and 1.0 $\times 10^{-7}$ mol/(m^2 s Pa) (equal to 1940, 1880 and 300 GPU) and mixture selectivities of 220, 45 and 22 through the best AlPO-18 membrane in equimolar CO_2/CH_4, CO_2/N_2 and H_2/CH_4 binary mixtures at room temperature and 0.2 MPa pressure drop, respectively. The effects of temperature and pressure on membrane separation performances in the three binary mixtures were discussed.

Introduction

The demands of separation and capture of light gases (e.g. CO_2 and H_2) for energy and environmental applications are rapidly increasing.[1] Both amine scrubbing used for CO_2 separation and cryogenic distillation used for H_2 separation are energy- and cost-intensive processes. Membrane technology can play a key role in making this separation economically feasible. Zeolite membranes with few defects can effectively separate light gases due to high separation performance, superior thermal and mechanical stabilities, and good chemical resistance in comparison with polymeric membranes.[2]

Cui *et al.*[3] prepared a zeolite T membrane and this membrane displayed CO_2/CH_4 selectivity of 400 and CO_2 permeance of 4.6×10^{-8} mol/(m^2 s Pa) at pressure drop of 0.1 MPa in equimolar CO_2/CH_4 mixture. Tomita *et al.*[4] reported that DDR membrane had CO_2/CH_4 selectivity of 280 and CO_2 permeance of 7×10^{-8} mol/(m^2 s Pa) for the same gas mixture. Surendar *et al.*[5] reported a ZIF-8 membrane with high CO_2 permeance [2.4×10^{-5} mol/(m^2 s Pa)], but the CO_2/CH_4 separation selectivities were only 4~7. Wang *et al.*[6] prepared a bilayer MFI membrane for high-temperature H_2/CO_2 separation with H_2 permeance of ~1.2×10^{-7} and H_2/CO_2 selectivity of 23 at 773 K.

Microporous aluminophosphates (AlPOs) are classes of zeolite materials built of equimolar AlO_4^- and PO_4^+ tetrahedral. The Si-substituted aluminophospate-34 (SAPO-34, CHA-type) membranes had CO_2/CH_4 selectivities of ~70 and CO_2 permeances of ~1.2×10^{-6} mol/(m^2 s Pa) for a feed pressure of 4.6 MPa.[7,8] The AlPO-42 (LTA-type) membranes showed a H_2/C_3H_8 selectivity of 146.[9] AlPO-18 has an AEI framework topology and a three-dimensional 8-ring channel system with a diameter of 0.38 nm.[10] It is an appealing membrane material for the separation of light gas mixtures because the small-pore AlPO-18 favors the diffusion of the smaller molecules such as H_2. Besides, AlPO-18 absorbs CO_2 more strongly than CH_4 and N_2,[11,12] which could improve separation performance in CO_2/CH_4 and CO_2/N_2 binary mixtures when it was used as membrane.

The reports on the synthesis of AlPO-18 films and membranes are yet rare.[13-16] Vilaseca *et al.*[13,14] prepared oriented AlPO-18 films on dense silicon wafers. Carreon *et al.*[15] prepared two-layer AlPO-18 membranes on the inside surface of tubular porous stainless steel tube supports by two-step secondary growth; the membranes displayed CO_2 permeances of ~7×10^{-8} mol/(m^2 s Pa) and CO_2/CH_4 selectivities of 52-60. Very recently, we have reported the synthesis of AlPO-18 membranes on the outer surface of symmetric α-alumina tubular supports by one-step secondary growth.[16] These membranes showed CO_2/CH_4 selectivities higher than 100 and CO_2 permeances of ~2×10^{-7} mol/(m^2 s Pa) in equimolar CO_2/CH_4 mixture.

The separation performance of a membrane was tightly related to the membrane microstructure including the morphologies of membrane layers, which were affected by synthesis conditions.[17] In this current study, the synthesis parameters for AlPO-18 membrane were optimized to reduce the membrane thickness and the growth of crystal into the support pore. Note that the symmetric alumina supports we used are much cheaper than the asymmetric ceramic supports[7,18] and the porous stainless steel supports.[15] The best AlPO-18 membrane in this study showed three times CO_2 permeance and doubled CO_2/CH_4 selectivities compared with our previous AlPO-18 membranes;[16] this membranes also had better integrated performance in the CO_2/CH_4 selectivity and CO_2 permeability than most of zeolite membranes.[3-5,8,15,16] The current AlPO-18 membranes were also used for the separations of CO_2/N_2 and H_2/CH_4 mixtures.

Experimental section

Membrane preparation

AlPO-18 membranes were synthesized on the outer surface of the symmetric porous α-alumina tubes by secondary growth. The molar compositions of the membrane gel were 1.0 Al_2O_3: 1.0 P_2O_5: x TEAOH: y H_2O, where TEAOH is tetraethylammonium hydroxide as template, x ranged from 1.5 to 2.2 (2 was the optimized value) and y ranged from 60 to 200 (160 was the optimized value). The synthesis gel were prepared by mixing aluminium isopropoxide (99%, Sigma-Aldrich), phosphoric acid

(85%, Sigma-Aldrich), TEAOH (35% in water, Sigma-Aldrich) and deionized water. After stirring the mixture for 6 h, a homogenous gel was obtained. The α-alumina tube supports (12-mm OD, 10-mm ID and 1.3-μm average pore size) from Nikkato Company were cut into 10-cm-long pieces and polished using 800# sandpaper, then washed several times with boiling DI water for 30 min and dried overnight at 373 K. After cleaning, the outer surface of the support tube was rubbed with the unclacined AlPO-18 seeds to implant the seeds on the surface of the support for nucleation. The nanosized AlPO-18 seeds were prepared according to the previously described procedure.[13,19] Two seeded supports were placed vertically in an autoclave and completely immersed in the membrane gel. The hydrothermal treatment was carried out in a conventional oven at 488 K for 14 h. After hydrothermal synthesis, the membranes were washed with flowing tap water for 15 min and dried overnight at 373 K. The membranes were calcined in the programed furnace in air at 723 K for 6 h with heating and cooling rates of 0.6 K/min. The calcined membranes were stored at 473 K prior to the separation tests.

Characterization and separation performance

AlPO-18 crystals and membranes were characterized using a field emission scanning electron microscopy (FE-SEM, Hitachi SU8020) at acceleration voltages of 5-10 KV. The crystal phases of the seeds and membranes were identified by XRD (Ultima IV) using Cu Kα radiation at 2-theta from 5° to 45° and a step size of 0.05°. Note that the membranes were not cut to make the XRD measurements.

Single-gas permeation was measured as a function of pressure and temperature using a dead-end (retentate stream blocked) system without sweep gas for four light gases (H_2, CO_2, N_2 and CH_4), similar to the measurements by Funke *et al.*.[20] The membranes were mounted in a stainless steel module, and sealed at each end with three silicone *O*-rings and two stainless steel rings. The feed gas flowed through the gap between the membrane and module and the permeate gas did through the inside of the tube. The ideal selectivity is the ratio of the single-gas permeances.

Mixed-gas separations in CO_2/CH_4, CO_2/N_2 and H_2/CH_4 binary mixtures through AlPO-18 membranes were measured without sweep gas, as described previously.[8,21] The feed flow rate was up to 8000 standard ml/min (SMLPM) to minimize concentration polarization.[22] The permeate pressure was kept to 0.103 MPa (absolute pressure; atmospheric pressure is 0.101 MPa). Mass flow controllers were used to control the molar ratio of each component. Each data point was obtained after a 2-h stabilization time, and changes in permeance of each component was lower than 3% in 1 h. The compositions of the feed and permeate streams were measured by a Shimadzu GC-2014C gas chromatograph with a thermal conductivity detector. A log-mean pressure drop is used for the calculation of the permeance. And the separation selectivity is the ratio of the permeances for mixtures. The permeability is the permeance multiplied by membrane thickness.

Modelling single CO_2 and CH_4 permeations in AlPO-18 membrane

The pressure dependence of the single-component CO_2 and CH_4 permeations were modelled assuming that CO_2 and CH_4 were all permeated through zeolite pores. The gas flux through a microporous membrane can be described by Maxwell-Stefan surface diffusion:

$$J = \frac{\rho q_{sat} D_{MS}}{L} \ln \frac{1-\theta_p}{1-\theta_f} \quad (1)$$

where, ρ is the zeolite density, L the effective thickness of the membrane, q_{sat} the saturation coverage and θ_f and θ_p are the fractional coverages in the feed and permeate. Single-component Maxwell-Stefan diffusivities were assumed to be coverage independent.[27] Eq. (1) can be written as:

$$J = \frac{\rho q_{sat} D_{MS}}{L} \ln \left(\frac{1+bp_f}{1+bp_p} \right) \quad (2)$$

where b is the adsorption equilibrium constant:

$$b = \exp\left(\frac{\Delta S}{R} - \frac{\Delta H_{ads}}{RT} \right) \quad (3)$$

Results and discussion

Membrane morphologies

AlPO-18 membrane morphologies were modified by optimizing synthesis conditions such as template concentration and gel dilution in order to increase the quality of AlPO-18 membrane (lower permeation resistance and lower defect concentration). The template-to-alumina ratio and gel dilution in this study are higher than those in our previous work.[16] $TEAOH/Al_2O_3$ and H_2O/Al_2O_3 ratios increased from 1.8 to 2 and 120 to 160, respectively. Fig. 1a shows the morphology of the cross section of the seeded supports. The seeds fully covered on the outer surface of the support with at least two layers. The surface SEM observation in Fig. 1b shows that the surface crystals of AlPO-18 membrane (M2) prepared under the optimized conditions had the cubic morphology, which was one of the typical morphology for AlPO-18 crystal[23] and AlPO-18 membrane.[16] Cross-sectional SEM image in Fig. 1c indicates that this membrane had a continuous crystal layer of about 8-μm thickness. The previous synthesis recipe resulted in a ~10-μm continuous top layer upon the same alumina support; besides, a lot of AlPO-18 crystals grew into the support pores with the depth of over 50 μm by SEM observations.[16] Different to the previous membrane,[16] the current membrane had few crystals inside support pores as seen in Fig. 1c, which could decrease the resistance of mass transfer and increase the permeation of molecules. As seen in Fig. 1a, the alumina support displayed the symmetric macropore structure with several micrometres in size. The larger void spaces through the surface to the body in symmetric supports were more suitable for crystal growth than the submicrometer pores in the asymmetric supports.[8] Thus, it was important to reduce the growth of crystals into the macropore when the symmetric supports were used. In the current study, the changes in gel compositions including the increases of template-to-alumina ratio and gel dilution improved the gel uniformity since aluminium isopropoxide dissolved more. The uniform gel prevent the particles in gel from depositing inside the pores of the supports and from becoming to the crystals, and therefore the permeance of the current membrane was higher. For the case of SAPO-34 membrane,[8] we also found that CO_2 permeance of SAPO-34 membrane was improved at a relatively higher $TEAOH/Al_2O_3$ ratio. When the $TEAOH/Al_2O_3$ ratio increased to 2.2, AlPO-18 membranes displayed poor CO_2/CH_4 selectivity probably because this base TEAOH gel (pH~9.5) could dissolve the membrane layer at high synthesis temperatures.[8] X-ray diffraction characterization in Fig. 1d further identified the seeds and the supported zeolite layers were pure AEI phase.

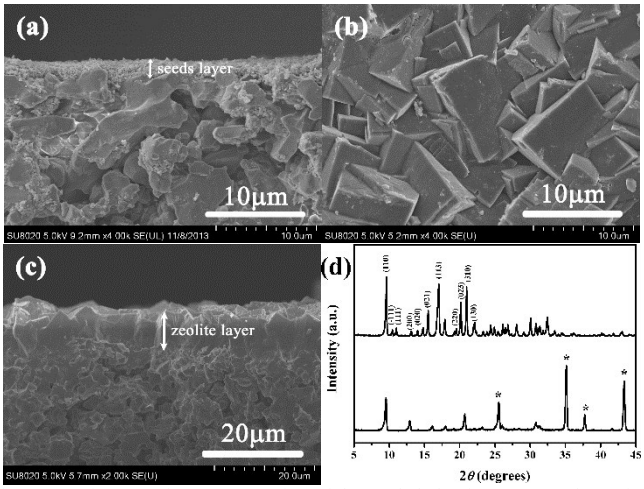

Fig. 1 SEM images of (a) cross-section of the seeded alumina support, (b) surface of alumina-supported AlPO-18 membrane (M5) and (c) cross-section of the AlPO-18 membrane (M5) and (d) XRD patterns of seeds (the upper) and AlPO-18 membrane (the bottom): ∗ represents the peaks of alumina supports.

The gel dilution affected the morphology and quality of AlPO-18 membranes. For example, a concentrated gel composition with a H_2O/Al_2O_3 ratio of 60 yielded the thick top layers of 30 μm with poor intergrowth, as shown in Fig. 2a. The thick and poor-packed membrane (M4) had the low permeance and poor selectivity [CO_2 permeance = 2.1×10^{7} mol/(m^2 s Pa) and CO_2/CH_4 selectivity = 60 in Table 1] in equimolar CO_2/CH_4 mixture at room temperature. The gel with H_2O/Al_2O_3 ratio of 200 were too diluted to grow a dense AlPO-18 membrane (M9), as shown in Fig. 2b (CO_2/CH_4 selectivity = 20 in Table 1).

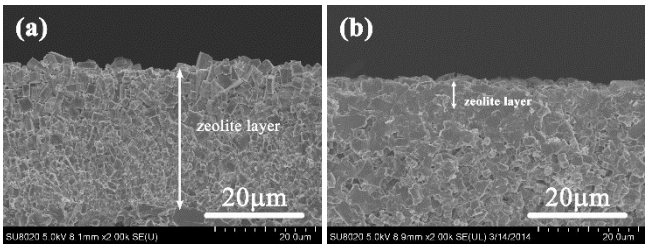

Fig. 2 Cross-sectional SEM images of the membranes prepared with H_2O/Al_2O_3 ratios of (a) 60 (M4) and 200 (M9), respectively.

Table 1 shows the permeation properties of AlPO-18 membranes prepared under different conditions in equimolar CO_2/CH_4 mixture at 298 K and 0.2 MPa pressure drop. The average CO_2 permeance and CO_2/CH_4 selectivity of four membranes (M2, M6-M8) under the optimized conditions were 6.3×10^{-7} mol/(m^2 s Pa) and 215, respectively. The standard deviations of CO_2 permeance and CO_2/CH_4 selectivity were 5.4% and 13.8%, respectively, indicating that membrane synthesis was reproducible. These membranes had twice higher permeances and better selectivities than our pervious AlPO-18 membranes[16] under the same test conditions. The differences in membrane morphologies between our current and previous membranes could be responsible to the difference in separation performance.

Table 1 Separation performances of AlPO-18 membranes prepared under different synthesis conditions in equimolar CO_2/CH_4 mixture at 298 K, 0.303 MPa feed pressure and 0.103 MPa permeate pressure.

No.	TEAOH/Al_2O_3 ratio (x value)	H_2O/Al_2O_3 ratio (y value)	CO_2 permeance$\times10^7$ [mol/(m^2 s Pa)]	CO_2/CH_4 selectivity
M1	1.8	160	4.1	160
M2	2.0	160	6.5	220
M3	2.2	160	20	8
M4	2.0	60	2.1	60
M5	2.0	120	4.6	140
M6	2.0	160	5.9	240
M7	2.0	160	6.3	210
M8	2.0	160	6.6	190
M9	2.0	200	11	20

Note: membrane gel compositions were 1.0 Al_2O_3: 1.0 P_2O_5: x TEAOH: y H_2O. Synthesis temperature and time were 488 K and 14 h, respectively.

Single-gas permeation

Single-gas permeances for H_2, CO_2, N_2, CH_4 and C_3H_8 measured at 298 K and 0.2 MPa pressure drop through AlPO-18 membrane (M2) are shown in Fig. 3. The permeances for the five gases decreased with the kinetic diameter of molecules except for CO_2. Carbon dioxide had the highest permeances, although H_2 is the smallest molecule. This is because CO_2 was strongly absorbed on AlPO-18.[12,24] From CO_2 to C_3H_8, the permeance significantly decreased with increasing molecular size, indicating that diffusivities of gas molecules decreased as their sizes approach the pore size of AlPO-18. The permeance of propane (kinetic diameter of 0.39 nm) is lower than the detection limit [1.0×10^{-11} mol/(m^2 s Pa)], indicating that the AlPO-18 membranes (pore size of 0.38 nm) have very low defect concentrations.

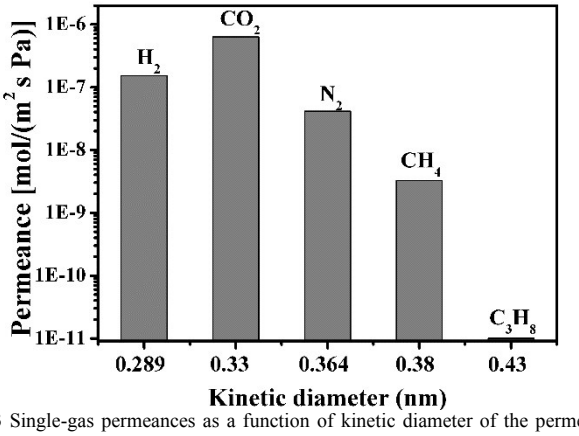

Fig. 3 Single-gas permeances as a function of kinetic diameter of the permeated molecules through AlPO-18 membrane M2 at 298 K, 0.301 MPa feed pressure and 0.101MPa permeate pressure. The lines are guides for eyes.

Fig. 4 illuminates temperature dependence of single-gas permeances for the four light gases through AlPO-18 membrane M2 at the temperature range from 298 to 423 K. The permeance of CO_2 decreased faster than that of CH_4 as temperature increased because the adsorption heats of CO_2 on AlPO-18 crystals is higher.[16] Hydrogen and CH_4 permeances had a minimum at 373 K. Bakker *et al.*[25] explained the behaviour of single-gas diffusion through zeolite membranes by a model that assumes the flux is the sum of surface diffusion and gas translational diffusion. The permeation of the adsorbed gas through zeolite pores decreased with increasing temperature until the permeation is primarily dominated by gas translation diffusion, so that the permeance has a minimum.

Temperature dependence of single-gas permeance in this membrane was analogous to that in SAPO-34 membrane[26] and in our previous AlPO-18 membrane.[16] Single CO_2 and H_2 permeances through membrane M2 at 298 K was 6.2×10^{-7} [= 1850 GPU (Gas Permeation Unit), 1GPU = 3.348×10^{-10} mol/(m^2·s·Pa)] and 1.5×10^{-7} mol/(m^2 s Pa) (= 450 GPU), respectively. The ideal CO_2/CH_4, CO_2/N_2 and H_2/CH_4 selectivities at 298 K were 200, 16 and 52, respectively. Both single CO_2 and H_2 permeances and the ideal selectivities through the current membrane were higher than our pervious membranes,[16] indicating that the quality of AlPO-18 membrane was improved after the synthesis optimization.

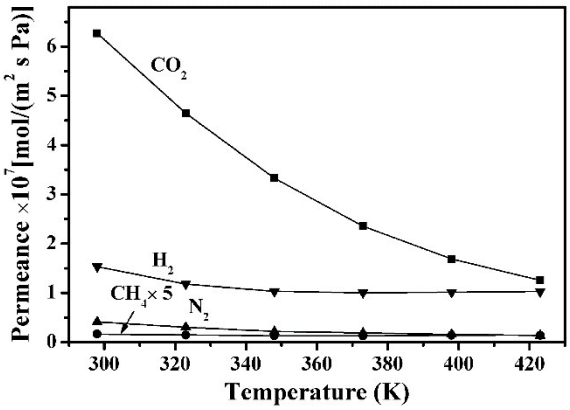

Fig. 4 Temperature dependence of single-gas permeances of H_2, CO_2, N_2 and CH_4 through AlPO-18 membrane M2 at 0.301 MPa feed pressure and 0.101MPa permeate pressure. The lines are guides for eyes. Note that CH_4 permeance was multiplied by 5 to make it easier to see.

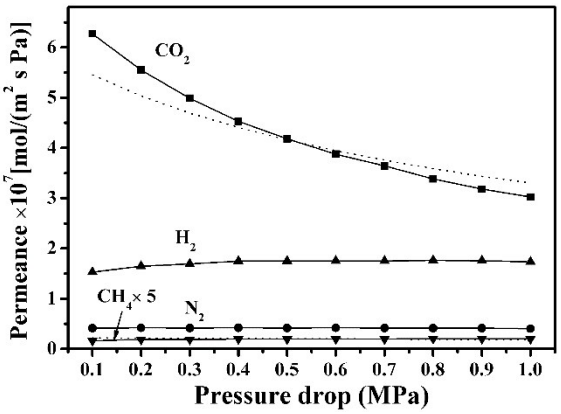

Fig. 5 Pressure dependence of single-gas permeances of H_2, CO_2, N_2 and CH_4 through AlPO-18 membrane M2 at 298 K and 0.101MPa permeate pressure. The symbols are measured permeances and the solid lines are guides for eyes. The dashed lines without symbols are predicted permeances by Eq. (2). Note that predicted and tested CH_4 permeances were multiplied by 5 to make it easier to see.

Single CO_2 permeance through AlPO-18 membrane (M2) also decreased with increasing pressure, as shown in Fig. 5. Single N_2, CH_4 and H_2 permeances were almost independent of or changed slightly with pressure. And thus the CO_2/CH_4, CO_2/N_2 and CO_2/H_2 ideal selectivities decreased with pressure.

Based on the adsorption equilibrium constant obtained from our previous adsorption test on AlPO-18 powders,[16] CO_2 and CH_4 permeances were predicted by Eq. (2) (dashed lines in Fig. 5). The Maxwell-Stefan diffusivity (D_{MS}) in Eq. (2) was assumed to be coverage independent.[27] The predicted permeances decreased because the chemical potential gradient of the adsorbed phase decreased as coverage approaches saturation at higher pressures. Carbon dioxide permeance decreases more than CH_4 permeance since the adsorption equilibrium constant (b) for CO_2 (0.024 kPa^{-1}) is greater than that for CH_4 (0.0042 kPa^{-1}). The measured CO_2 permeances fit the predicted ones except at the lowest pressure drop. In contrast, the measured CH_4 permeances did not decrease (but increased slightly) with pressure drop as predicted, although they were close to the predicted values. Flow through non-zeolite pores was previously used to explain this behaviour.[27]

Separation of light gas mixtures

Separation performances of AlPO-18 membranes were evaluated using the typical three CO_2/CH_4, CO_2/N_2 and H_2/CH_4 binary mixtures. Fig. 6 shows the CO_2/CH_4 selectivity and permeance through membrane M2 in equimolar CO_2/CH_4 mixture as a function of temperature at 0.303 MPa feed pressure and 0.103 MPa permeate pressure. The single-gas permeations for CO_2 and CH_4 were also included in Fig. 6. The mixture CO_2 permeance decreased with temperature and CH_4 permeance was independent of temperature, resulting in the decrease in CO_2/CH_4 selectivities with temperature. At lower temperature of 298 K, the mixture CO_2/CH_4 selectivity was higher than ideal CO_2/CH_4 selectivity. But it was lower at temperatures higher than 323 K because the mixture CH_4 permeance increased faster. Membrane M2 displayed a CO_2 permeance of 6.5×10^{-7} mol/(m^2 s Pa) (= 1940 GPU) and CO_2/CH_4 selectivity of 220 at 298 K in equimolar CO_2/CH_4 mixture. Fig. 7 shows pressure dependence of the permeance and selectivity through membrane M2 at 298 K. Mixture CH_4 permeance was lower than single CH_4 permeance and mixture CO_2 permeance was higher than single CO_2 permeance at the pressure range at 298 K. Thus, mixture CO_2/CH_4 selectivity was higher than ideal selectivity.

Keizer *et al.*[28] modelled two component permeation through zeolite MFI membranes, in which both molecular sizes and the relative adsorption strengths are considered to determine the faster permeating species in a binary mixture. The CO_2 specie had faster diffusion (smaller molecular size) and higher coverage (higher adsorption amount) in AlPO-18 membrane than CH_4 specie did, and thus CO_2 permeates faster through zeolite pores. As temperature increases, the coverage of CO_2 decreased dramatically, which results in the decrease of selectivity. At low temperatures, preferential adsorption of CO_2 (high-coverage specie) could inhibit CH_4 (low-coverage specie) adsorption and increase the mixture CO_2/CH_4 selectivity.[26] Thus, the separation selectivity was higher than the ideal selectivities at low temperatures. The separation selectivity dropped faster than idea selectivity because the coverage of CO_2 in the mixture decreased faster as temperature increased.

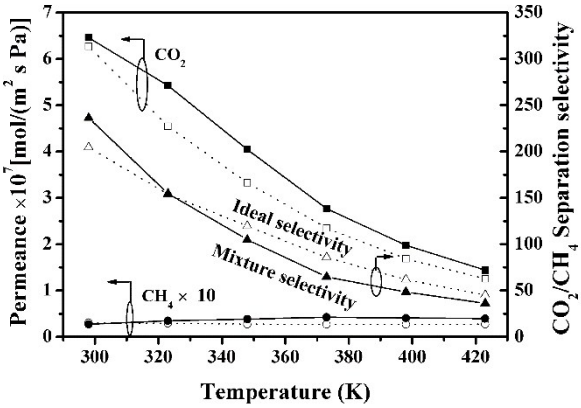

Fig. 6 Temperature dependence of selectivity and permeance through AlPO-18 membrane (M2) in equimolar CO_2/CH_4 mixture at 0.303 MPa feed pressure and 0.103 MPa permeate pressure. Single-gas permeance and ideal selectivity are shown for comparison. The solid symbols represent the data in mixtures and the open ones represent the data in single gas. The lines are guides for eyes.

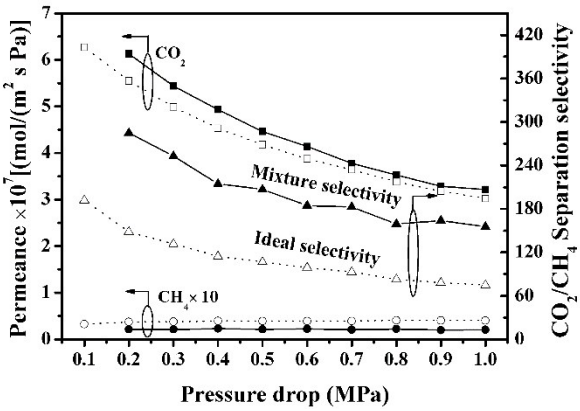

Fig. 7 Pressure dependence of selectivity and permeance through AlPO-18 membrane (M2) in equimolar CO_2/CH_4 mixture at 298 K and 0.103 MPa permeate pressure. Single-gas permeance and ideal selectivity are shown for comparison. The solid symbols represent the data in mixtures and the open ones represent the data in single gas. The lines are guides for eyes.

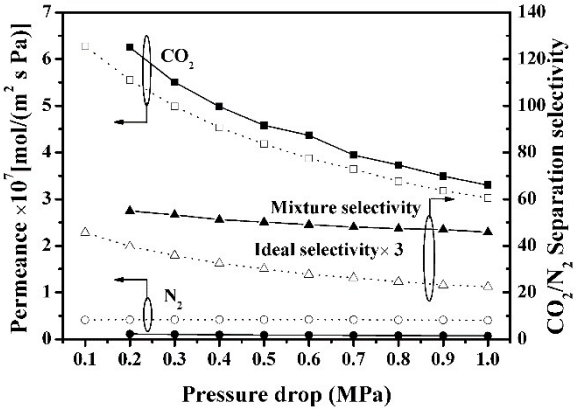

Fig. 9 Pressure dependence of selectivity and permeance through AlPO-18 membrane (M2) in equimolar CO_2/N_2 mixture at 298 K and 0.103 MPa permeate pressure. Single-gas permeance and ideal selectivity are shown for comparison. The solid symbols represent the data in mixtures and the open ones represent the data in single gas. The lines are guides for eyes.

Fig. 8 shows temperature dependence of separation performance through AlPO-18 membrane M2 in equimolar CO_2/N_2 mixture at 0.303 MPa feed pressure and 0.103 MPa permeate pressure. At low temperatures, mixture N_2 permeance (the slow diffusion specie) were lower than the single N_2 permeance, leading to the fact that mixture CO_2/N_2 selectivity was higher than ideal CO_2/N_2 selectivity. Similar to that in CO_2/CH_4 mixture (in Fig. 6), mixture selectivity in CO_2/N_2 mixture decreased faster than ideal selectivity as temperature increased, Fig. 9 illuminates pressure dependence of separation performance in CO_2/N_2 mixture using the same membrane at 298 K. Similar to those in CO_2/CH_4 mixture (in Fig. 7), the permeance of faster permeating specie (CO_2) decreased with pressure and the permeance of the other specie (N_2) was independent of pressure. At 298 K and 0.2 MPa pressure drop, CO_2 permeance and CO_2/N_2 selectivity in equimolar CO_2/N_2 mixture through AlPO-18 membrane (M2) were 6.3×10^{-7} mol/(m^2 s Pa) (= 1880 GPU) and 45, respectively.

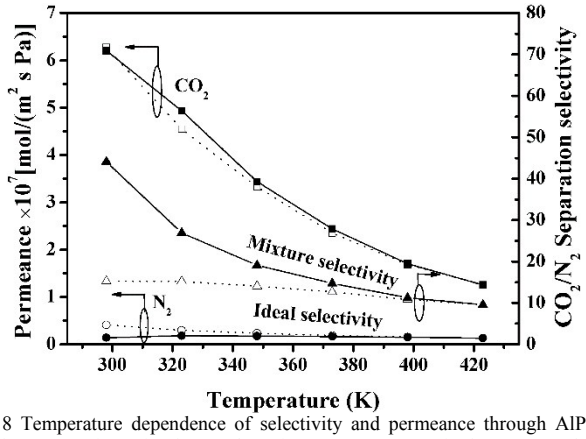

Fig. 8 Temperature dependence of selectivity and permeance through AlPO-18 membrane (M2) in equimolar CO_2/N_2 mixture at 0.303 MPa feed pressure and 0.103 MPa permeate pressure. Single-gas permeance and ideal selectivity are shown for comparison. The solid symbols represent the data in mixtures and the open ones represent the data in single gas. The lines are guides for eyes.

Temperature and pressure dependences of separation performance through AlPO-18 membrane (M2) in equimolar H_2/CH_4 mixture were shown in Figs. 10 and 11, respectively. Mixture H_2 permeance had a maximum and single H_2 permeance had a minimum with temperature. Mixture CH_4 permeance was higher than single CH_4 permeance, leading to a lower mixture H_2/CH_4 selectivity. Mixture H_2 permeance decreased with pressure and mixture CH_4 was independent of pressure, as shown in Fig. 11. Hydrogen permeance and selectivity in H_2/CH_4 mixture (in Fig. 11) were lower than single H_2 permeance and H_2/CH_4 ideal selectivity, which was opposite to those in CO_2/CH_4 and CO_2/N_2 mixtures (in Figs. 7 and 9). This is because that the adsorption of H_2 on AlPO-18 membrane is too weak to inhibit CH_4 permeation. In contrast, CH_4 permeation inhibited H_2 permeation and decreased H_2 permeance and H_2/CH_4 selectivity in the mixture. Single H_2 permeance increased a little at low pressures in Fig. 11, which was different to the permeation by Langmuir model, in which H_2 permeance is expected to be constant at low pressure. It could attribute to the flow of nonzeolite pore. Nonzeolite pores were normally larger than the zeolite pore and allowed Knudsen and viscous flow.[26] These flows were increased by the partial pressure of molecules. Similar results were reported in SAPO-34 membranes.[26] At 298 K and 0.2 MPa pressure drop, H_2 permeance and H_2/CH_4 selectivity through AlPO-18 membrane (M2) in equimolar H_2/CH_4 mixture were 1.0×10^{-7} mol/(m^2 s Pa) (= 300 GPU) and 22, respectively.

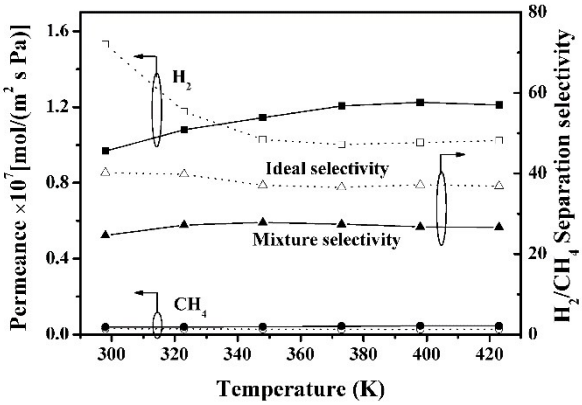

Fig. 10 Temperature dependence of selectivity and permeance through AlPO-18 membrane (M2) in equimolar H_2/CH_4 mixture at 0.303 MPa feed pressure and 0.103 MPa permeate pressure. Single-gas permeance and ideal selectivity are shown for comparison. The solid symbols represent the data in mixtures and the open ones represent the data in single gas. The lines are guides for eyes.

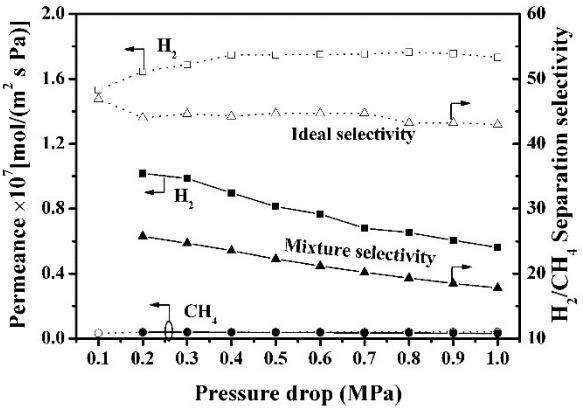

Fig. 11 Pressure dependence of selectivity and permeance through AlPO-18 membrane (M2) in equimolar H_2/CH_4 mixture at 298 K and 0.103 MPa permeate pressure. Single-gas permeance and ideal selectivity are shown for comparison. The solid symbols represent the data in mixtures and the open ones represent the data in single gas. The lines are guides for eyes.

Comparison to the literatures

Figs. 12 and 13 compare our AlPO-18 membrane with polymeric membranes presented in the CO_2/CH_4 and H_2/CH_4 separation Robeson plots,[29] respectively. A membrane thickness of 8 μm verified from the SEM image in Fig. 2c was used in calculating the permeability (permeance multiplied by membrane thickness). The AlPO-18 membrane exceeded the upper bounds observed for polymer membranes and the thermally rearranged (TR) polymeric membranes for both CO_2/CH_4 and H_2/CH_4 mixtures.

Several kinds of zeolite membranes in CO_2/CH_4 separation were included in Fig. 12 for comparison. AlPO-18,[15,16] zeolite T[3] and DDR[4] membranes were reported to be ~10 μm thick. SAPO-34 membranes were 5 and 3 μm thick when stainless steel support[30] and asymmetric alumina support[8] were used, respectively. Zeolite membranes all exceeded the upper bounds. The current AlPO-18 membrane had better integrated performance in the CO_2/CH_4 selectivity and CO_2 permeability than most of zeolite membranes.[3,4,8,15,16,30] Note that the permeance of asymmetric alumina-supported SAPO-34 membranes[8] was higher than that of this AlPO-18 membrane because of the thinner membrane thickness. The current symmetric alumina membrane supports are much cheaper than the asymmetric membrane supports.[8,18]

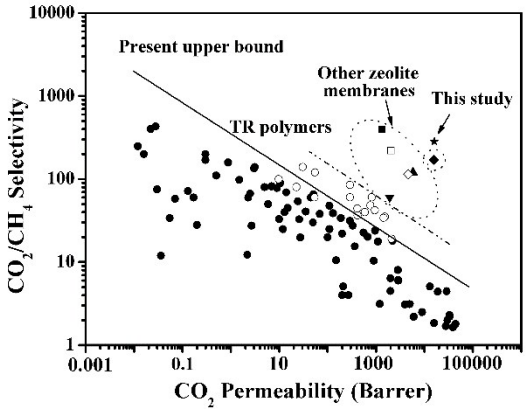

Fig. 12 Comparison of our AlPO-18 membrane (M2) with polymeric membranes presented in the CO_2/CH_4 separation Robeson plot.[29] Other zeolite membranes are included for comparison. ■: zeolite T membrane;[3] □: DDR membrane;[4] ▼,▲: AlPO-18 membranes[15,16] and ♦,◊: SAPO-34 membranes.[8,30]

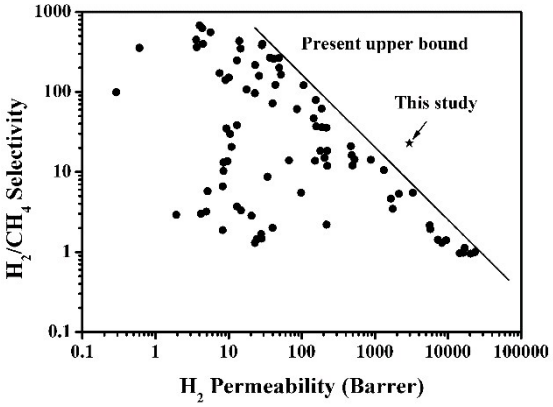

Fig. 13 Comparison of our AlPO-18 membrane (M2) with polymeric membranes presented in the H_2/CH_4 separation Robeson plot.[29]

Conclusions

Continuous AlPO-18 membranes with low defect concentrations were synthesized using low-cost symmetric alumina supports by optimizing the synthesis conditions. Single-gas permeances of CO_2, N_2, CH_4 and C_3H_8 decreased with increasing kinetic diameter. The measured single CO_2 and CH_4 permeances dependence of pressure drop were in close agreement with that predicted from the Maxwell-Stefan diffusion model. The best AlPO-18 membrane had the smaller-component permeances of 6.5, 6.3 and 1.0 $\times 10^{-7}$ mol/(m^2 s Pa), and mixture selectivities of 220, 45 and 22 for equimolar CO_2/CH_4, CO_2/N_2 and H_2/CH_4 mixtures, respectively, at 298 K and 0.2 MPa pressure drop. Carbon dioxide and H_2 permeances decreased as pressure increased in the three mixtures. Carbon dioxide permeance decreased in CO_2/CH_4 and CO_2/N_2 mixtures, but H_2 permeance increase in H_2/CH_4 mixture as temperature increased.

Acknowledgements

We gratefully acknowledge the supports by National Natural Scientific foundation of China (contract numbers: 21366013 and 21490585).

Notes and references

[a] State Key Laboratory of Materials-Oriented Chemical Engineering, College of Chemistry and Chemical Engineering, Nanjing Tech. University, Nanjing 210009, China
[b] College of Chemistry and Chemical Engineering, Jiangxi Normal University, Nanchang 330022, China
* Corresponding author: rf-zhou@njtech.edu.cn

1 M. Yu, R.D. Noble, J.L. Falconer, *Acc. Chem. Res.*, 2011, **44**, 1196.
2 Y.S. Lin, M.C. Duke, *Curr. Opin. Chem. Eng.*, 2013, **2**, 209.
3 Y. Cui, H. Kita, K.-i. Okamoto, *J. Mater. Chem.*, 2004, **14**, 924.
4 T. Tomita, K. Nakayama, H. Sakai, *Micropor. Mesopor. Mater.*, 2004, **68**, 71.
5 S.R. Venna, M.A. Carreon, *J. Am. Chem. Soc.*, 2009, **132**, 76.
6 H.B. Wang, X.L. Dong, Y.S. Lin, *J. Membr. Sci.*, 2014, **450**, 425.
7 E.W. Ping, R. Zhou, H.H. Funke, J.L. Falconer, R.D. Noble, *J. Membr. Sci.*, 2012, **415-416**, 770.
8 R.F. Zhou, E.W. Ping, H.H. Funke, J.L. Falconer, R.D. Noble, *J. Membr. Sci.*, 2013, **444**, 384.

9 A. Huang, F. Liang, F. Steinbach, T.M. Gesing, J. Caro, *J. Am. Chem. Soc.*, 2010, **132**, 2140.
10 A. Simmen, L.B. McCusker, C. Baerlocher, W.M. Meier, *Zeolites*, 1991, **11**, 654.
11 L. Predescu, F.H. Tezel, S. Chopra, *Adsorption*, 1997, **3**, 7.
12 Q.L. Liu, N.C.O. Cheung, A.E. Garcia-Bennett, N. Hedin, *ChemSusChem*, 2011, **4**, 91.
13 M. Vilaseca, S. Mintova, V. Valtchev, T.H. Metzger, T. Bein, *J. Mater. Chem.*, 2003, **13**, 1526.
14 M. Vilaseca, S. Mintova, K. Karaghiosoff, T.H. Metzger, T. Bein, *Appl. Surf. Sci.*, 2004, **226**, 1.
15 M.L. Carreon, S. Li, M.A. Carreon, *Chem. Commun.*, 2012, **48**, 2310.
16 T. Wu, B. Wang, Z. Lu, R. Zhou, X. Chen, *J. Membr. Sci.*, 2014, **471**, 338.
17 Z. Lai, G. Bonilla, I. Diaz, J.G. Nery, K. Sujaoti, M.A. Amat, E. Kokkoli, O. Terasaki, R.W. Thompson, M. Tsapatsis, D.G. Vlachos, *Science*, 2003, **300**, 456.
18 N. Kosinov, C. Auffret, C. Gucuyener, B.M. Szyja, J. Gascon, F. Kapteijn, E.J.M. Hensen, *J. Mater. Chem. A*, 2014, **2**, 13083.
19 H. van Heyden, S. Mintova, T. Bein, *J. Mater. Chem.*, 2006, **16**, 514.
20 H.H. Funke, B. Tokay, R. Zhou, E.W. Ping, Y. Zhang, J.L. Falconer, R.D. Noble, *J. Membr. Sci.*, 2012, **409**, 212.
21 Y. Zheng, N. Hu, H. Wang, N. Bu, F. Zhang, R. Zhou, *J. Membr. Sci.*, 2015, **475**, 303.
22 A.M. Avila, H.H. Funke, Y. Zhang, J.L. Falconer, R.D. Noble, *J. Membr. Sci.*, 2009, **335**, 32.
23 R. Wendelbo, D. Akporiaye, A. Andersen, I.M. Dahl, H.B. Mostad, *Appl. Catal. A-Gen*., 1996, **142**, L197.
24 I. Deroche, L. Gaberova, G. Maurin, P. Llewellyn, M. Castro, P. Wright, *Adsorption*, 2008, **14**, 207.
25 W.J.W. Bakker, L.J.P. Van Den Broeke, F. Kapteijn, J.A. Moulijn, *AIChE J.*, 1997, **43**, 2203.
26 J.C. Poshusta, V.A. Tuan, E.A. Pape, R.D. Noble, J.L. Falconer, *AIChE J.*, 2000,**46**, 779.
27 S. Li, J.L. Falconer, R.D. Noble, *J. Membr. Sci.*, 2004, **214**, 121.
28 K. Keizer, A.J. Burggraaf, Z.A.E.P. Vroon, H. Verweij, *J. Membr. Sci.*, 1998, **147**, 159.
29 L.M. Robeson, *J. Membr. Sci.*, 2008, **320**, 390.
30 S. Li, J.L. Falconer, R.D. Noble, *Adv. Mater.*, 2006, **18**, 2601.

A table of contents entry

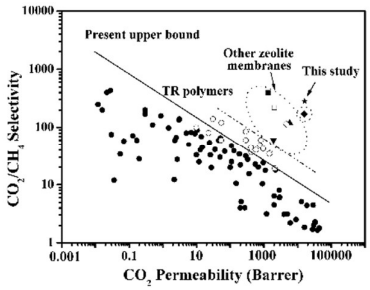

AlPO-18 membranes synthesized using lost-cost symmetric alumina supports showed high performance for light gas separation beyond most of zeolite membranes.